Facile Preparation of Dibenzoheterocycle-Functional Nanoporous Polymeric Networks with High Gas Uptake Capacities

ARTICLE *in* MACROMOLECULES · MAY 2014

Impact Factor: 5.8 · DOI: 10.1021/ma500080s

8 AUTHORS, INCLUDING:

Guipeng Yu
Central South University
37 PUBLICATIONS **268** CITATIONS
SEE PROFILE

Jianguo Guan
Wuhan University of Technology
194 PUBLICATIONS **2,378** CITATIONS
SEE PROFILE

Xiang Xiong
Central South University
162 PUBLICATIONS **1,150** CITATIONS
SEE PROFILE

Zhonggang Wang
Dalian University of Technology
500 PUBLICATIONS **10,264** CITATIONS
SEE PROFILE

Macromolecules

Article

pubs.acs.org/Macromolecules

Facile Preparation of Dibenzoheterocycle-Functional Nanoporous Polymeric Networks with High Gas Uptake Capacities

Shaofei Wu,[†] Yao Liu,[†] Guipeng Yu,*[,†] Jianguo Guan,[‡] Chunyue Pan,*[,†] Yong Du,[§] Xiang Xiong,[§] and Zhonggang Wang*[,∥]

[†]College of Chemistry and Chemical Engineering, Central South University, Changsha 410083, China

[‡]State Key Laboratory of Advanced Technology for Materials Synthesis and Processing, Wuhan University of Technology, Wuhan 430070, China

[§]State Key Laboratory of Powder Metallurgy, Central South University, Changsha 410083, China

[∥]State Key Laboratory of Fine Chemicals, Department of Polymer Science & Materials, Dalian University of Technology, Dalian 116012, China

Supporting Information

ABSTRACT: A consolidated ionothermal strategy was developed for the polymerization of thermally unstable nitriles to construct high performance materials with permanent porosity, and carbazole, dibenzofuran, and dibenzothiophene were separately introduced into covalent triazine-based networks to investigate the effects of heterocycles on the gas adsorption performance. Three nitriles, namely 3,6-dicyanocarbazole, 3,6-dicyanodibenzofuran, and 3,6-dicyanodibenzothiophene, were designed and synthesized, which were readily converted to heat-resistant intermediates at a moderate temperature and then polymerized to create highly porous poly(triazine) networks instead of the traditional one-step procedure. This documents an improved strategy for the successful construction of heterocyclic-functional triazine-based materials. The chemical structures of monomers and polymers were confirmed by ^{1}H NMR, FTIR, and elemental analysis. Such polymers with high physical−chemical stability and comparable BET surface areas can uptake 1.44 wt % H_2 at 77 K/1 bar and 14.0 wt % CO_2 at 273 K/1 bar and present a high selectivity for gas adsorption of CO_2 (CO_2/N_2 ideal selectivity up to 45 at 273*K*/1.0 bar). The nitrogen- and oxygen-rich characteristics of carbazole and dibenzofuran feature the networks strong affinity for CO_2 and thereby high CO_2 adsorption capacity. This also helps to thoroughly understand the influence of pore structure and chemical composition on the adsorption properties of small gas molecules.

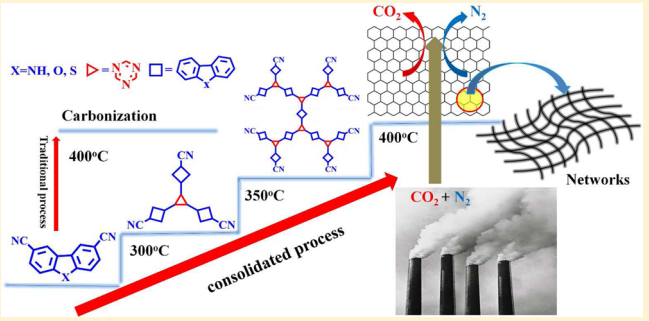

INTRODUCTION

One of the most urgent challenges facing energy sector is the mitigation of greenhouse gases implicated in global warming.[1] Although some technologies including amine scrubbing and cryogenic separation are already available for CO_2 capture, the substantial energy consumptions required for CO_2 release for sequestration and regeneration of the amine solutions together with severe corrosion of equipment limit their popularity.[2] Adsorption by porous solids (such as zeolite, metal−organic frameworks, etc.), featuring large capacity and low cost, was deemed as the promising and competitive method for CO_2 recovery.[3] However, the main drawback of such cation-containing sorbents is their low tolerance to water vapor that is usually present in the gas stream.[4] The water molecules with dipole moments will preferentially interact with the cations, thus significantly damaging the popularity of such CO_2 sorbents.[5]

Recently, a new type of substitute for traditional porous sorbents, namely porous organic polymers (POPs),[6] has been constructed from various pure organic building blocks via robust covalent bonds. High stability (thermal and chemical), low skeletal density, and multitudinous structural modification methods enable POPs to be promising candidates for CO_2 sorbents.[7] Major research efforts are currently focused on a rational design of POPs to combine the CO_2-sorption capacity and selectivity as well as good reversibility of POPs under ambient conditions.[8] Two factors should be taken into account for a high performance CO_2 sorbent. First, narrow ultramicropores (<1 nm) make a greater contribution to CO_2 adsorption than wide micropores and mesopores, considering thermodynamic size of CO_2,[9] which can be ascribed to the fact that the former enhances the filling by the CO_2 molecule.[8c,10] Second, the acceptable binding energy between host and guest CO_2 molecule would enable the strong but reversible adsorption−desorption.[11] For the second concern, one of the

Received: January 10, 2014
Revised: April 27, 2014

   dx.doi.org/10.1021/ma500080s | Macromolecules XXXX, XXX, XXX−XXX

most extensively studied and effective strategies is the introduction of polar functional moieties onto the pore surface either through the *pre*optimization of building blocks or using *post*modification method.[12] Typically, the network A disclosed by Cooper et al., which is composed of neat benzene rings, can uptake CO_2 of 2.65 mmol g^{-1} at 273 K and 1 bar, while triazole-functional network C exhibits a remarkably improved CO_2 uptake capability (3.86 mmol g^{-1}).[13] Han et al. constructed microporous polycarbazole (COP-1) with a high uptake capacity for CO_2 (21.2 wt %) and a moderate CO_2/N_2 adsorption selectivity (25).[14] Exciting CO_2 capture performance close to those required for either pre- or postcombustion capture is also demonstrated by polyamine and sulfonate-grafted PPN-6s,[15] oxygen-rich phloroglucinol-based porous polymers,[16] nitrogen-rich microporous polybenzimidazoles,[7a,17] nitrogen- and oxygen-rich microporous cyanate resins,[18] etc. As common commercially available materials, carbazole, dibenzothiophene, and dibenzofuran are suitable blocks for building porous organic polymers due to their unique electroactivity and useful photophysical property. In these cases, the introduction of dibenzoheterocycles makes the polymer electron-rich, and hence this approach appears promising in improving isosteric heat of adsorption and gas adsorption capability. In addition, each of the dibenzoheterocycles contains two phenyl rings but connected by a different heterocyclic core. Thus, after cross-linking, the polar surface in the networks could be systematically varied while same topologies will be obtained because of similar initial structure, which enables us to examine the influence of pore structure and chemical composition on the adsorption capacity and selectivity toward small gas molecules.

As a special and emerging class of POPs, covalent triazine-based frameworks (CTFs) were first developed utilizing dynamic trimerization reaction in $ZnCl_2$ ionothermal conditions by Kuhn et al. Although only CTF-1 shows same interesting crystalline properties as COF-1, a new cheap method to obtain porous CTFs from abundant, thermally stable organic nitriles was developed.[19] However, much harsher reaction conditions (reaction temperatures >400 °C) have to be applied to enable the reversible formation of triazines.[20] This completely destroys the polymerization feasibility of a large number of building blocks with heterocyclic moieties (e.g., carbazole and thiophene) that are easily broken down but deliver a great positive effect to gas adsorption ability. Impressive technologies such as the microwave-assisted method by Qiu and Cooper and acid catalysis by Liu known as high efficiency, however, do not fundamentally hamper the thermal decomposition and acidolysis.[21] Aromatic nitriles can cyclotrimerize to thermally stable phenyl-*s*-triazine derivatives with the aid of acid at moderate temperatures. The basis of this outstanding work goes back to several contributions by Marvel and Huang which described the instantaneous formation of polytriazine oligomers of low polymerization degree under the catalysis of $ZnCl_2$.[22] This has initiated our efforts to develop a flexible strategy to construct high performance networks with permanent porosity from such nitrile blocks.

Inspired by these works, a consolidated ionothermal strategy (instead of traditional one-step procedure) for the building of functional CTFs from three temperature-unstable monomers was demonstrated. We introduce carbazole, an extensively employed moiety, and two uninvestigated units, namely dibenzofuran and dibenzothiophene, into covalent triazine-based frameworks. Our study also aims to demonstrate the influence of dibenzoheterocyclic units on the selective CO_2 adsorption for the first time.

EXPERIMENTAL SECTION

Materials. Dibenzofuran, dibenzothiophene, carbazole, and copper(I) cyanide were purchased from Aladdin Chemical Inc. and used as received. Zinc chloride was refluxed and distilled over thionyl chloride to remove water, and then excess thionyl chloride was azeotropically distilled with toluene. After the removal of thionyl chloride and toluene, anhydrous zinc chloride was obtained after being dried at 180 °C under vacuum for 24 h. Unless otherwise specified, all other solvents and reagents were purchased from Energy Inc. and used as received.

Characterization Methods. FT-IR spectra were collected with a VARIAN 1000 FT-IR (scimitar series) spectrometer in the 400−4000 cm^{-1} region (KBr pressed disks). Thermogravimetric analysis (TGA) was performed at a heating rate of 10 K/min under N_2 or air atmosphere using a PerkinElmer TGA 7. ^1H NMR (400 MHz) spectra were obtained with a Bruker spectrometer at an operating temperature of 25 °C using DMSO-d_6 or $CDCl_3$ as solvents, and the data were listed in parts per million downfield from tetramethylsilane (TMS). ^{13}C NMR (100 MHz) spectra were obtained with a Bruker spectrometer at an operating temperature of 25 °C. CHN analysis was performed on a Vario ELIII CHNOS Elementaranalysator from Elementaranalysesysteme GmbH. Wide-angle powder X-ray diffraction (WAPXRD) data were collected over the 2θ range 5°−60° on a CPS120 Inel diffractometer equipped with Ni-filtered Cu Kα radiation (40 kV, 100 mA) at room temperature with a scan speed of 5° min^{-1}. High-resolution transmission electron microscopy (HR-TEM) images were collected in a JEOL JEM-2100F microscope at an accelerating voltage of 200 kV. Prior to TEM measurement, the sample was ultrasonically dispersed in ethanol and dropped onto a copper grid coated with a carbon film. Scanning electron microscopy (SEM) experiments were performed on a FEI Quanta-200 scanning electron microscope. The dry state polymer surface areas and pore size distributions were performed at a Micromeritics ASAP 2020 sorption analyzer by nitrogen adsorption and desorption at 77 K. The specific surface areas (BET) were calculated according to the BET model in the relative pressure (P/P_0) ranging from 0.01 to 0.1. Pore size distributions were derived from the N_2 adsorption isotherms using the NLDFT (nonlocal density functional theory) method. CO_2 adsorption isotherms were measured at 273 and 298 K up to 1.0 bar, while H_2 adsorption isotherms were measured at 77 and 87 K with the same pressure scale. High-purity gas (99.999%) was used for adsorption experiments. Prior to the measurements, the samples were degassed at 200 °C under high vacuum for 12 h.

Synthesis of Monomers. *3,6-Dibromocarbazole.* A 500 mL round-bottomed flask was charged with carbazole (8.4 g, 50 mmol) and chloroform (300 mL), and a solution of Br_2 (5.15 mL, 105 mmol) in 50 mL of chloroform was added at 0 °C drop by drop. The mixture was stirred at 0 °C for another 1 h and then transferred to room temperature for another 12 h. The resultant mixture was poured into 1000 mL of sodium bicarbonate solution (1 mol/L), and the organic phase was separated off and dried over anhydrous sodium sulfate. The volume of the solution was reduced by rotary vaporization. After recrystallization by ethanol, a crystalline pale red solid (13.3 g) was obtained. Yield: 82%; mp: 204−206 °C. ^1H NMR ($CDCl_3$): 8.07−8.11 (s, 2H), 7.48−7.56 (d, 2H), 7.24−7.32 (d, 2H).

3,6-Dicyanocarbazole. 3,6-Dibromocarbazole (6.5 g, 20 mmol) and cuprous cyanide (8.89 g, 100 mmol) were charged, and then 250 mL of dry DMF was injected by syringe under an N_2 atmosphere. After being stirred at 150 °C for 48 h, the reaction mixture was poured into a cold solution of 100 g of ferric chloride in 150 mL of concentrated hydrochloric acid and stirred for another 2 h. The brown solid was collected by filtration, washed with water and ethanol several times, and dried under vacuum. The obtained crude product was chromatographed on a silica gel column with petroleum ether/dichloromethane as eluent, and a white solid (1.5 g) was obtained. Yield: 35%. ^1H NMR (DMSO): 8.16−8.18 (s, 2H), 7.72−7.78 (d, 2H), 7.64−7.7 (d, 2H).

3,6-Dibromodibenzofuran. The synthesis procedure of 3,6-dibromodibenzofuran was almost the same as for 3,6-dibromocarbazole.

dx.doi.org/10.1021/ma500080s | *Macromolecules* XXXX, XXX, XXX−XXX

The product was obtained as a white solid. Yield: 89%; mp: 226−227 °C. ^{1}H NMR ($CDCl_3$): 8.0−8.04 (s, 2H), 7.55−7.59 (d, 2H), 7.42−7.46 (d, 2H).

3,6-Dicyanodibenzofuran. 3,6-Dicyanodibenzofuran was prepared in almost the same procedure as for 3,6-dicyanocarbazole. The product was obtained as a pale yellow solid. Yield: 39%. ^{1}H NMR ($CDCl_3$): 8.31−8.35 (s, 2H), 7.84−7.86 (d, 2H), 7.74−7.78 (d, 2H).

3,6-Dibromodibenzothiophene. 3,6-Dibromodibenzothiophene was prepared in almost the same procedure as for 3,6-dibromocarbazole. The product was obtained as a white solid. Yield: 79%; mp: 225−227 °C. ^{1}H NMR ($CDCl_3$): 8.23−8.25 (s, 2H), 7.69−7.74 (d, 2H), 7.56−7.6 (d, 2H).

3,6-Dicyanodibenzothiophene. 3,6-Dicyanodibenzothiophene was prepared in almost the same procedure as for 3,6-dicyanodibenzofuran. The product was obtained as a pale yellow solid. Yield: 31%. ^{1}H NMR ($CDCl_3$): 8.48−8.5 (s, 2H), σ = 8−8.04 (d, 2H), σ = 7.78−7.82 (d, 2H).

Synthesis of NPTNs. *NPTN-1a.* NPTN-1a was synthesized by heating a mixture of 3,6-dicyanocarbazole (0.3 g, 1.4 mmol) and $ZnCl_2$ (1.84 g, 14 mmol) in a quartz tube (3 × 5 cm) according to the literature.[7c,23] The tube was evacuated to a high vacuum and then sealed rapidly. Following by a temperature program (250 °C/10 h), the quartz tube was cooled to room temperature, and the reaction mixture was subsequently ground and then washed thoroughly with water to remove the catalyst. A yellow solid was obtained. Yield: 99%.

NPTN-1b. The synthesis procedure of NPTN-1b was similar to that for NPTN-1a, except a different temperature program (250 °C/10 h, 300 °C/10 h) was applied during the heating cycles. A brown solid was obtained. Yield: 98%.

NPTN-1c. The synthesis procedure of NPTN-1c was similar to that for NPTN-1a, except a different temperature program (250 °C/10 h, 300 °C/10 h, 350 °C/10 h) was applied during the heating cycles. A black solid was obtained in a yield of 98%.

NPTN-1d. For the synthesis of NPTN-1d, a traditional synthetic method in which the monomer was heated to 400 °C by one step was utilized. Unfortunately, at the first time the reaction in a quartz tube (3 × 5 cm) was suspended suddenly due to a blast of the tube after 10 h heating program (supposing to be 40 h). The method was repeated twice by changing the size of quartz tube (3 × 10 cm), and then a black solid was obtained after removing the catalyst by water. Yield: 62% (2nd) and 64% (3rd).

NPTN-1. NPTN-1 was synthesized by heating a mixture of the synthesized 3,6-dicyanocarbazole (0.3 g, 1.4 mmol) and $ZnCl_2$ (1.84 g, 14 mmol) in a quartz tube (3 × 5 cm). The tube was evacuated to a high vacuum and then sealed rapidly. Following by a temperature program (250 °C/10 h, 300 °C/10 h, 350 °C/10 h, 400 °C/20 h), the quartz tube was cooled to room temperature, and the reaction mixture was subsequently ground and then washed thoroughly with water to remove most of the catalyst. Further stirring in diluted HCl for 15 h was carried out to remove the residual salt. The resulting black powder was filtered and washed successively with water and methyl alcohol, followed by an overnight Soxhlet extraction using acetone, methyl alcohol, and hexane as eluting solvent sequentially, and finally dried in vacuum at 150 °C. Yield: 94%.

NPTN-2. Synthesis procedure of NPTN-2 was almost the same as for NPTN-1, and a black solid was obtained starting from 3,6-dicyanodibenzofuran. Yield: 96%.

NPTN-3. Synthesis procedure of NPTN-3 was almost the same as for NPTN-1, and a black solid was obtained starting from 3,6-dibromodibenzothiophene. Yield: 93%.

RESULTS AND DISCUSSION

A series of covalent triazine-based frameworks (CTFs) were obtained successfully from the abundant organic nitriles such as *o*-DCB (1,2-dicyanobenzene), *p*-DCB, *m*-DCB, and 4,4′-dicyanobiphenyl (DCBP) reported by Kuhn and Antonietti,[19,24] 1,3,5-tricyanobenzene by Thomas,[7c] 2,6-naphthalenedicarbonitrile (NDC) by Bojdys,[25] supramolecule tetranitrile and (1,3-bis-, 1,3,5-tris-), 1,3,5,7-tetrakis(4-cyanophenyl)adamantine by Janiak,[23,26] and 1,4-dicyano-2,3,5,6-tetrafluorobenzene by Han.[27]

Notably, all monomers motioned above are thermally stable to endure continuous heating at 400 °C or even at other higher temperatures (600 °C). To probe this feasibility, TGA measurements (Figure S1, Supporting Information) on the three monomers were conducted prior to the polymerization. The highest decomposition temperature (T_d, recorded as the temperature for 10 wt % mass loss under N_2 atmosphere) was recorded at 350 °C by 3,6-dicyanodibenzofuran, while those of the others (3,6-dicyanodibenzothiophene: T_d = 250; 3,6-dicyanocarbazole: T_d = 252 °C) are much lower relative to previous disclosed building blocks such as *o*-DCB, DCBP, and NDC (T_d > 400 °C).[19] Additionally, our results demonstrated that the traditional synthetic technology by which the monomer was heated to 400 °C by one step leads to almost complete carbonization, while that using trifluoromethanesulfonic acid as catalyst under room temperature has caused breakage within C−N and C−O linkages of the nitrile monomers (Table S1, Supporting Information). This definitely hampers the facile construction of high performance porous materials and their wide applications as small gas sorbents.

For comparison, different heating cycles were applied to the polymerization of the carbazole-functional nitriles. The specific synthetic results were displayed in Table S1. As described, heating at reaction temperatures of less than 350 °C mainly yielded deep yellow or brown organosoluble products (NPTN-1a,b,c) which are supposed to be low-molecular-weight compounds. By one-step heating the monomer 3,6-dicyanocarbazole to 400 °C in the traditional procedure a black insoluble material (NPTN-1d) was obtained. As expected, only networks with high degree of carbonation were obtained, accompanying with the extremely low yield (62%) and high nitrogen loss as shown by element analysis (Table S2). Fourier infrared spectrum analysis was chosen to probe the deeper structure variations of the materials. NPTN-1a displays almost the same features to the initial monomers implying a low-level trimerization. As shown in Figure S2, the expected intermediates were generated after heating at around 300 °C (NPTN-1b). Typically, after polymerization at 300 °C, the intensity of nitrile absorption at about 2235 cm^{-1} is about 39% of the origin intensity of 3,6-dicyanocarbazole, while it is around 24% of the origin intensity after curing at 350 °C (NPTN-1c), normalized to the =C−H stretch band at 3066 cm^{-1} (Figure S3). Additionally, a gradual increase of absorption intensity at round 1360 and 1510 cm^{-1} indicates a remarkably improved conversion with an increasing reaction temperature. Thermogravimetric analysis (TGA) under a N_2 atmosphere displayed in Figure 1 demonstrates a superior stability compared to the initial monomers. As depicted, after

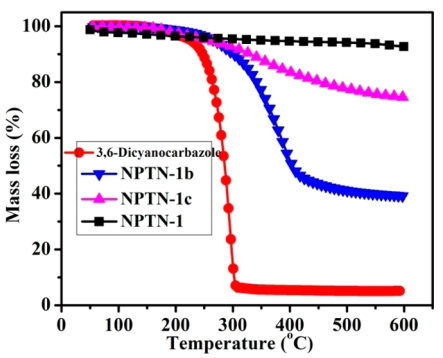

Figure 1. TGA thermograms of 3,6-dicyanocarbazole and NPTN-1 under different heating cycles.

dx.doi.org/10.1021/ma500080s | *Macromolecules* XXXX, XXX, XXX−XXX

Scheme 1. Synthesis Routes to NPTNs

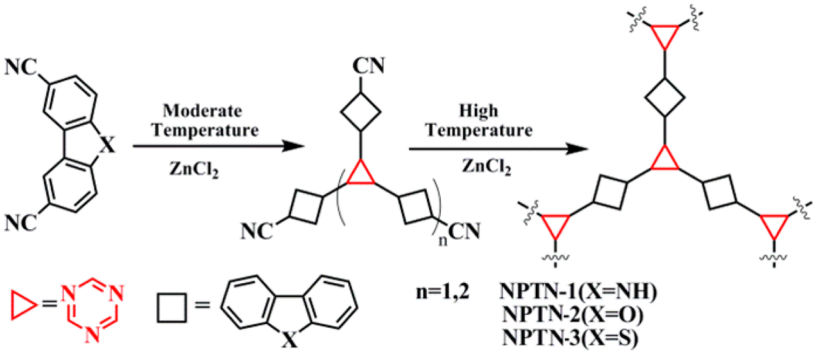

polymerization at 300 °C, 10 wt % mass loss temperature of the obtained network (NPTN-1b) has been promoted from 250 to 305 °C. With further heating at 350 °C, the T_d of the resultant network (NPTN-1c) was raised to 350 °C. Black and highly cross-linked polymers (NPTN-1) were obtained by heating NPTN-1c at the temperature of 400 °C for another 20 h. In addition to a higher yield (>90%) than NPTN-1d, we assume that thermally unstable nitriles were readily converted to heat-resistant intermediates as we expected, while the carbonation has been suppressed effectively.

Herein, the novel series of nanoporous triazine-based networks (NPTNs) functioned by dibenzoheterocyclic units (i.e., carbazole, dibenzofuran, and dibenzothiophene) were synthesized from aromatic nitriles in sealed quartz ampules via a modified dynamic reaction (Scheme 1). For the preparation of NPTNs, a kind of stable intermediates can be synthesized in molten $ZnCl_2$ under moderate temperatures, prior to the generation of the target product. Such intermediates, namely prepolymers with low polymerization degrees (e.g., trimer, pentamer), are not highly cross-linked but stable enough for high reaction temperatures comparing to the initial monomers. The low-molecular-weight compounds without any pore characteristics can be easily resolved by the Lewis acid. When a higher reaction temperature is used, highly cross-linked polymers will be readily obtained in quantitative yields under ionothermal conditions.

The obtained networks are insoluble in any common organic solvents such as dimethyl sulfoxide (DMSO), *N*,*N*-dimethylformamide (DMF), *N*,*N*-dimethylacetamide (DMAc), *N*-methylpyrrolidone (NMP), and tetrahydrofuran (THF), along with diluted HCl solution (10 wt %), implying a physical−chemical stable hyper-cross-linked nature. The stability test was further examined by refluxing NPTNs in diluted HCl solution (10 wt %) for 5, 20, and 48 h, and neither color change nor weight loss was observed. The recovered networks were evaluated after acid soaking using nitrogen sorption experiments at 77 K. The apparent surface area values calculated from Brunauer−Emmett−Teller (BET) models are all kept comparing with the original networks. It is worth mentioning that the nitrogen loss as evidenced by the elemental analysis (EA in Table S2) is low, which is consistent with other studies.[19,20] TGA thermograms under air condition deliver excellent thermostability of NPTNs with 10 wt % weight loss at round 470 °C (Figure S2). The T_d values of NPTN-1−3 were raised by 220, 230, and 120 °C compared with those of the corresponding monomers determined under N_2 atmosphere, respectively. The significantly promoted stability is most possibly resulted from the strong charge transfer interactions between the formed *s*-triazine rings and dibenzoheterocyclic units. This physical and chemical stability is higher than MOFs (unstable to heat), molecular sieve (unstable to acid), and COFs, etc.,[3d,28] and comparable to other POPs such as HCPs,[29] CMPs,[1c,30] PIMs,[31] etc., endowing the network application value under a harsh environment.[32]

The chemical connectivity and the structure of NPTNs were characterized by Fourier transform infrared (FT-IR), solid ^{13}C CP/MAS NMR spectra. As illustrated in FT-IR spectra (Figures S3−S5), the disappearance of intense C≡N band at about 2230 cm^{-1} is indicative of a high conversion of nitriles, while the appearance of strong absorption bands at round 1360 (C−N) and 1510 cm^{-1} (C═N) and a signle peak at 173 ppm (C in *s*-triazine) in the solid ^{13}C NMR spectrum (Figure S6) suggests the successful formation of triazine. The other major peaks observed at 138 and 129 ppm could be assigned to the substituted aromatic carbon bonded to nitrogen atom and substituted aromatic carbon of aromatic ring connected with triazine ring, respectively.[33] Morphologies study of NPTNs by SEM demonstrates aggregates of uniform and compact microgel particles with a size of 100−200 nm. A dark and bright area can be clearly observed from HR-TEM images, confirming a porous characteristic, while the intermediates NPTN-1c and NPTN-1d present a dense and compact surface on the SEM/TEM images implying nonporous nature. As shown in Figure S17, the isotherm of NPTN-1c and NPTN-1d display almost no uptake under low relative pressure (P/P_0 < 0.2) and slight uptake up to P/P_0 = 0.99, confirming nonporous nature. PXRD spectra of NPTNs are featureless, suggesting their amorphous nature (Figure S18). Briefly, three hyper-cross-linked polymers with good thermal and physical−chemical stability were constructed from temperature-unstable nitriles by the step-by-step ionothermal method.

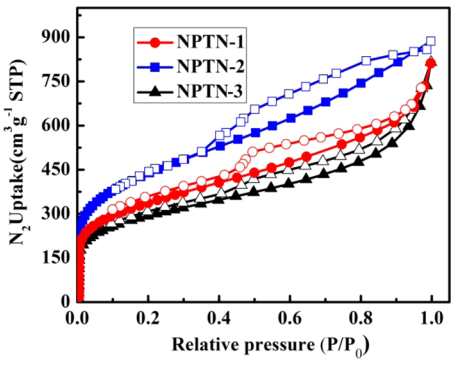

Figure 2. Nitrogen sorption isotherms of NPTNs at 77 K.

dx.doi.org/10.1021/ma500080s | *Macromolecules* XXXX, XXX, XXX−XXX

The nitrogen adsorption isotherms exhibit a sharp uptake in the low pressure region ($P/P_0 < 0.01$), implying a significant microporosity for the networks, whereas the isotherms also demonstrate the presence of mesoporous for another relative steady rise phase ranges from 0.2 to 0.8 (P/P_0).[34] All three networks show significant increase of nitrogen uptake over 0.8 (P/P_0), suggesting the presence of macroporous structure. This can be interpreted as the interparticulate voids arising from the loose packing of small particles as observed in the SEM micrographs. The desorption isotherms display a typical desorption−adsorption hysteresis, which is ascribed to the softness of organic polymer skeleton and swelling effect in critical nitrogen.

BET surface area values calculated from relative pressure between 0.01 and 0.1 were listed on Table 1. NPTN-2 shows the highest BET area of 1558 m^2/g with a total pore volume (V_t, P/P_0 = 0.9 bar) up to 1.23 cm^3/g, while the BET surface area and total pore volume for NPTN-1 (1187 m^2/g, 0.93 cm^3/g) and NPTN-3 (1055 m^2/g, 0.83 cm^3/g) are not much of a difference but slightly lower relative to NPTN-2. Although the surface areas and pore volumes were lower than those of most COFs and PAFs,[35] these values are still comparable with many other organic adsorbents.[18a,36]

Table 1. Pore Parameters for NPTNs

polymer	SA_{BET}[a] (m^2/g)	V_{Total}[b] (cm^3/g)	$V_{0.1}$[c] (cm^3/g)	$V_{0.1}/V_t$
NPTN-1	1187	0.93	0.44	47.3
NPTN-2	1558	1.23	0.57	46.3
NPTN-3	1055	0.83	0.39	47

[a]Calculated using adsorption branches over the pressure range 0.01−0.1 bar of N_2 isotherm at 77 K. [b]Determined from the N_2 isotherm at P/P_0 = 0.90 bar. [c]Determined from the N_2 isotherm at P/P_0 = 0.1 bar.

Using nitrogen as probe, the experimental pore size distributions for the NPTNs networks were obtained from the adsorption isotherms by the nonlocal density functional theory (NLDFT).[37] It is interesting to observe that all the samples have almost same microporous and mesoporous sizes. Figure 3 shows that a large fraction of pores originating from microspores with a diameter less than 20 Å range from 0.35 to 0.71 nm and 1.1 to 2.0 nm, while a considerable proportion of mesopores is broadly distributed from 20 to 50 Å. The fraction of microporosity was compared by the ratio of micropore volume to total pore volume ($V_{0.1}/V_t$), where $V_{0.1}$ refers to the pore volume calculated from N_2 nitrogen sorption at 0.1 bar and V_t at 0.9 bar. Notably, NPTN-2 has the highest total pore volume of 1.23 cm^3/g, while its microporosity fraction ($V_{0.1}/V_t$) was the least (47.3%, 46.3%, and 47% for NPTN-1, NPTN-2, and NPTN-3, respectively).

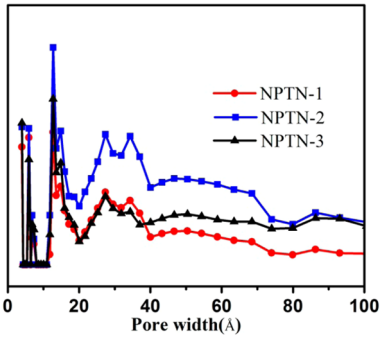

Figure 3. NLDFT pore size distribution curves of NPTNs.

The CO_2 adsorption isotherms at 273 and 298 K (Figure 4) demonstrated that the absorbed amount continually increased with the rising pressure, implying that the adsorptions have not reached their equilibrium or saturated state in the pressure range investigated. Among the porous materials, dibenzofuran-functional NPTN-2 exhibits the highest CO_2 uptake of 14.0 wt % at 273 K and 6.9 wt % at 298 K (1 bar) for its dominant high BET surface area, while the corresponding value for NPTN-1 containing carbazole moiety is slightly lower of 13.3 and 8.1 wt %. These uptakes are comparable to many impressive examples like PAF-18-OLi (14.4 wt %, 273 K, 1 bar),[12b] triptycene-based microporous poly(benzimidazole) networks TBI-1 (14.0 wt %, 273 K, 1 bar),[17b] and nanoporous porphyrin polymers Ni-Por-1 (13.8 wt %, 273 K, 1 bar),[36a] but lower than PAF-1-CH_2NH_2 (about 19.4 wt %, 273 K, 1 bar)[35b] and covalent triazine frameworks CTF-0 (15.7 wt %, 273 K, 1 bar).[7c] This high CO_2 uptake capacity might be attributed to the presence of heterocylics and strong polar surface interaction between the network and guest gas molecule. Caused by low polarity of sulfur atom and hence weak interaction, NPTN-3 shows the minimum uptake capacities (9.8 wt %) in spite of its comparable specific surface area and pore volume to NPTN-2. Because of the rich nitrogen content, this capacity is still competitive with those of many reported porous organic polymers with higher BET surface, such as furan-based imine-linked POF-1 (7.7 wt %, 273 K, 1 bar),[38] porous borazine-linked polymers BLP-1H (7.8 wt %, 273 K, 1 bar),[39] and microporous cyanate resin CE-2 (7.9 wt %, 273 K, 1 bar).[18a] With comparable surface area and pore volume, it is usually envisioned that the N, O in NPTNs create a high electric field on the network surface, leading to a high binding force with quadrupolar CO_2 molecules. Notably, NPTN-1 has a higher CO_2 uptake than NPTN-2 in the range of 0.01−0.6 bar as evidenced by the sorption isotherms. This may indicate that efficient doping of nitrogen helps to achieve a high CO_2 uptake at low pressure regions, while doping of oxygen prefers to enhance adsorption at relatively high pressure.[9b,40] As a result, the CO_2 capacities for the investigated NPTNs are not highly related to its surface area but closely related to the surface nature.

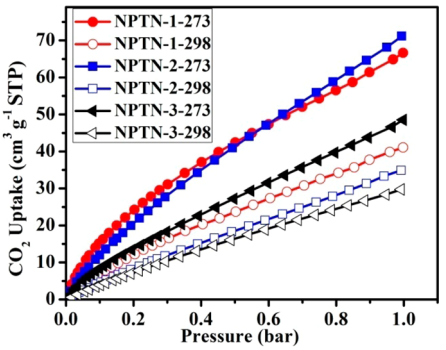

Figure 4. CO_2 adsorption isotherms of NPTNs at 273 and 298 K.

To gain further insights from the host−guest interaction, Q_{st} (CO_2 isosteric heat of adsorption) was obtained with the Clausius−Clapeyron equation from the CO_2 adsorption isotherms at 273 and 298 K.[41] All materials show a high Q_{st} for CO_2 (>30 kJ/mol) (Figure 5) at low coverage, and the Q_{st} is lower than MOF materials of CuBTTri which possesses the highest Q_{st} for CO_2 (96 kJ/mol) and MRF (>40 kJ/mol),[42] but it

dx.doi.org/10.1021/ma500080s | Macromolecules XXXX, XXX, XXX−XXX

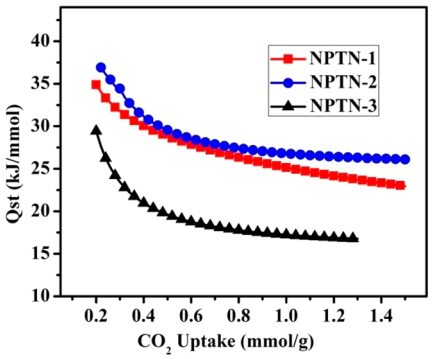

Figure 5. Isosteric heat of adsorption of CO_2 versus the uptake amount.

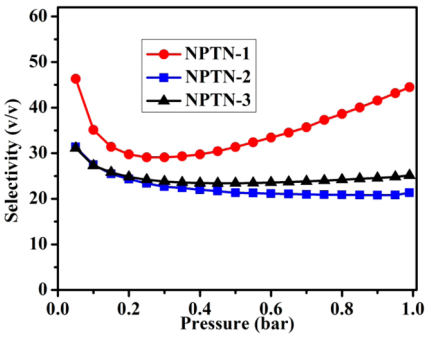

Figure 6. IAST selectivity of NPTNs for CO_2 (0.15 bar) over N_2 (0.85 bar).

is of the same level to many other POPs based on heterocyclic rings, such as HCP-1 (23.5 kJ/mol),[43] CMP networks (27.0−33.0 kJ/mol), and COFs (15−30 kJ/mol).[44] As shown in Figure 5, the values are arranged in the following order: NPTN-2 (37 kJ/mol) > NPTN-1 (34 kJ/mol) > NPTN-3 (30 kJ/mol), which is consistent with that of the CO_2 capacities. Comparatively strong interactions of guest molecules with the adsorbent walls, which are heats of adsorption, are necessary for CO_2 adsorption. Besides, other microporous parameters include pore shape, degree of disorder, internal surface chemistry, or the free volume also play a role in CO_2 sorption properties. A steeper downward trend of the Q_{st} value for NPTN-1 leads to a weaker interaction with CO_2 than NPTN-2 with the increasing capacities. The CO_2 adsorption of NPTN-3 is lower than that of NPTN-1 and NPTN-2, which mainly can be attributed to the tiny contribution from heats of CO_2 adsorption. Generally, isosteric heat of adsorption will be affected by the interaction between intersorbate and pore space, or the size distinctions between pore size distributions and adsorbed molecules and so on.[45] From these viewpoints, the difference of CO_2 capacities and isosteric heat value can be explained. First, there are some differences among the surface of three polymers. The incorporation of triazine and heterocyclics with abundant nitrogen and oxygen atom endow NPTN-1 and NPTN-2 high surface polarity, which significantly enhance their affinity for CO_2. Most possibly because of the largest physical polarity of oxygen, NPTN-2 exhibits the highest Q_{st} value along with the highest capacity for CO_2. Meanwhile, sulfur atom does a little contribution to the interaction of the network with CO_2, resulting the lowest Q_{st} value and CO_2 uptake of NPTN-3. Second, the presence of ultramicropores always means a strong affinity toward gas molecules, and hence such porous materials show high gas uptakes at low pressures due to the overlap of the potential fields from both sides of the pore walls.

To assess the potential in gas separation, some accounts can be taken by considering CO_2/N_2 selectivity. For evaluation of realistic *post*combustion capture of CO_2, selectivity of CO_2 over N_2 at an equilibrium partial pressure of 0.85 bar (N_2) and 0.15 bar (CO_2) in the bulk phase was imitated by ideal adsorbed solution theory (IAST) model according to many other studies by the equation[15b,46]

$$S_{i/j} = \frac{x_i/x_j}{y_i/y_j}$$

where the idea selectivity refers to the first component over the second, and x_i, x_j and y_i, y_j denote the molar fractions of species i, j in the adsorbed and bulk phases, respectively. Adsorption isotherms for both CO_2 and N_2 are shown in Figures S19−24 at 273 K for pressures of 0−1 bar. NPTN-1−3 exhibit a pronounced CO_2 uptake and a fairly low N_2 adsorption at pressure <1 bar. The different adsorption ability toward CO_2 and N_2 provides a basis for the selective capture of CO_2 from gas-mixture streams. CO_2/N_2 selectivity depends on two aspects, including the capacities of carbon dioxide and nitrogen. Both improving CO_2 and reducing N_2 uptakes will be beneficial for the raise of selectivity. Typically, the CO_2 uptake abilities at 273 K/1 bar were 3.01 mmol/g (13.3 wt %) for NPTN-1 and 3.18 mmol/g (14.0 wt %) for NPTN-2, respectively. The corresponding values for N_2 uptake were 0.126 mmol/g (3.58 wt %) and 0.177 mmol/g (4.96 wt %) at the same condition, respectively. NPTN-1 displays a higher ideal selectivity (45) than NPTN-2 (22) for a larger decrease of N_2 uptake (1.38 wt %) than CO_2 uptake (0.7 wt %). Here, a low uptake of N_2 might be the controlling factor. NPTN-3 exhibits the lowest CO_2 capacities but also the lowest N_2 uptake (0.109 mmol/g), and hence the ideal selectivity is a litter higher than NPTN-2 of 25 (Table 2).

Table 2. Summary of CO_2 Uptakes for NPTNs

polymer	$CO_2^{273\ K}$ (wt %)	$CO_2^{298\ K}$ (wt %)	Q_{st} (kJ/mol)	selectivity[a]
NPTN-1	13.3	8.1	34	45
NPTN-2	14.0	6.9	37	22
NPTN-3	9.8	5.9	30	25

[a]Calculated by the IAST model from 85% N_2 and 15% CO_2 at 273K and 1 bar.

The obtained ideal selectivity is comparable to many other POPs,[46b,47] and NPTN-1 overrates all other CTFs disclosed. This suggests that the introduction of carbazole has significantly improved the selectivity of CTFs. The high CO_2/N_2 selectivity of NPTN-1 can be attributed to the stronger interaction with CO_2 molecule than N_2. The presence of triazine groups and strong polar surface accelerates the interactions with the polarizable CO_2 molecules through dipole−quadrupole interactions. Meanwhile, NPTN-1 shows weaker affinity toward N_2 comparing to NPTN-2 and other CTFs. Similar to −N=N− reported, carbazole moieties display some N_2-phobic like nature.[11a] However, possibly due to both strong affinity toward CO_2 and N_2 molecular, NPTN-2 shows the lowest ideal selectivity in spite of its highest CO_2 uptake. Although NPTN-2 has a marginally higher CO_2 uptake than NPTN-1, it has a lower CO_2 uptake and a higher N_2 adsorption in the low pressure region, which makes NPTN-1 a promising candidate for postcombustions.

At 77 K and 1 bar, NPTN-2 exhibits 1.44 wt % hydrogen uptake (Figure S25). Similar to the CO_2 isotherms, the H_2 uptake

dx.doi.org/10.1021/ma500080s | *Macromolecules* XXXX, XXX, XXX−XXX

has not reached saturation in the investigated pressure range, implying that high storage can be expected at higher pressures. The high adsorption capacity of NPTN-2 can refer to its polar surface due to the presence of triazine ring and oxygen atom. The adsorption enthalpy is always claimed to be the most effective parameter at low loadings for hydrogen storage at 77 K.[48] Typically, the Q_{st} value of NPTN-2 (Figure S26) decreases to within the range 4−9.6 kJ mol^{-1} at higher hydrogen uptake, which is typical for dispersive van der Waals interactions. It is worthwhile to note that the Q_{st} value of NPTN-2 at low coverage is up to 9.6 kJ/mol, and the NPTN has a comparably high hydrogen uptake at 1 bar and 77 K than most of the other porous polymers reported so far.[49]

CONCLUSIONS

In summary, we developed a consolidated ionothermal polymerization procedure for the synthesis of three new nanoporous triazine-based networks (NPTN-1,2,3) functioned by varying dibenzoheterocyclic units (i.e., carbazole, dibenzofuran, and dibenzothiophene). Comparing with the traditional one-step method (NPTN-1d), the novel modified polymerization procedure is proved to be more suitable for the construction of nanoporous polymers derived from temperature-unstable nitriles. The resulting networks synthesized by this strategy display much better physical−chemical stability than their monomers and comparable high BET surface areas in the range of 1055−1558 m^2/g. The polymers demonstrated adsorption capacities under normal pressures up to 1.44 wt % for H_2 at 77 K and 1 bar, 14.0 wt % CO_2 for carbon dioxide at 273 K and 1 bar, respectively. High gas adsorption selectivities were also obtained with the value over 45 (v/v, 273 K) in an ideal CO_2/N_2 system. The introduction of carbazole, dibenzofuran, and dibenzothiophene enhanced the heats of adsorption and uptakes of gases such as CO_2 and H_2. In addition, POPs modified by carbazole unites probably showed weak affinity toward N_2 and displayed high gas adsorption selectivities for the CO_2/N_2 system. Such observations may be particularly useful in developing heterocyclic-based POPs for gas storage and separation.

ASSOCIATED CONTENT

Supporting Information

Two tables and 33 figures, including the synthetic process and results, FTIR and ^1H NMR spectra of aromatic cyanide monomers, FTIR, solid-state ^{13}C CP/MAS NMR spectra, PXRD patterns, SEM images, HRTEM images, TGA curves, and hydrogen adsorption isotherm as well as the date of elemental analysis and adsorption selectivities of CO_2 over N_2 of the dibenzoheterocycle-functional nanoporous polymeric networks. This material is available free of charge via the Internet at http://pubs.acs.org.

AUTHOR INFORMATION

Corresponding Authors

*E-mail gilbertyu@csu.edu.cn (G.P.Y.).
*E-mail zgwang@dlut.edu.cn (Z.G.W.).

Author Contributions

S.W. and Y.L. contributed to this work equally.

Notes

The authors declare no competing financial interest.

ACKNOWLEDGMENTS

We acknowledge the financially support from the National Science Foundation of China (Nos. 21204103 and 21376272), Hunan Provincial Natural Science Foundation of China (13JJ413), China Postdoctoral Science (2012M521535), State Key Laboratory of Advanced Technology for Materials Synthesis and Processing (2012-KF-14), and State Key Laboratory of Fine Chemicals (KF1206).

REFERENCES

(1) (a) Liu, C.; Fan, Y. Y.; Liu, M.; Cong, H. T.; Cheng, H. M.; Dresselhaus, M. S. *Science* **1999**, *286*, 1127−1129. (b) Leaf, D.; Verolme, H. J. H.; Hunt, W. F. *Environ. Int.* **2003**, *29*, 303−310. (c) Xu, Y.; Jin, S.; Xu, H.; Nagai, A.; Jiang, D. *Chem. Soc. Rev.* **2013**, *42*, 8012−8031. (d) Yang, H. Q.; Xu, Z. H.; Fan, M. H.; Gupta, R.; Slimane, R. B.; Bland, A. E.; Wright, I. *J. Environ. Sci. (Beijing, China)* **2008**, *20*, 14−27.

(2) (a) Wu, Z.; Li, W.; Xia, Y.; Webley, P.; Zhao, D. *J. Mater. Chem.* **2012**, *22*, 8835−8845. (b) Goeppert, A.; Czaun, M.; Prakash, G. S.; Olah, G. A. *Energy Environ. Sci.* **2012**, *5*, 7833−7853. (c) Rochelle, G. T. *Science* **2009**, *325*, 1652−1654.

(3) (a) Thiruvenkatachari, R.; Su, S.; An, H.; Yu, X. X. *Prog. Energy Combust. Sci.* **2009**, *35*, 438−455. (b) Hao, G. P.; Li, W. C.; Qian, D.; Lu, A. H. *Adv. Mater.* **2010**, *22*, 853−857. (c) Li, J.-R.; Ma, Y.; McCarthy, M. C.; Sculley, J.; Yu, J.; Jeong, H.-K.; Balbuena, P. B.; Zhou, H.-C. *Coord. Chem. Rev.* **2011**, *255*, 1791−1823. (d) D'Alessandro, D. M.; Smit, B.; Long, J. R. *Angew. Chem., Int. Ed.* **2010**, *49*, 6058−6082. (e) Ma, S. Q.; Zhou, H. C. *Chem. Commun.* **2010**, *46*, 44−53.

(4) Merel, J.; Clausse, M.; Meunier, F. *Ind. Eng. Chem. Res.* **2008**, *47*, 209−215.

(5) (a) Kaye, S. S.; Dailly, A.; Yaghi, O. M.; Long, J. R. *J. Am. Chem. Soc.* **2007**, *129*, 14176−14177. (b) Czaja, A. U.; Trukhan, N.; Müller, U. *Chem. Soc. Rev.* **2009**, *38*, 1284−1293.

(6) (a) Cote, A. P.; Benin, A. I.; Ockwig, N. W.; O'Keeffe, M.; Matzger, A. J.; Yaghi, O. M. *Science* **2005**, *310*, 1166−1170. (b) Wood, C. D.; Tan, B.; Trewin, A.; Niu, H. J.; Bradshaw, D.; Rosseinsky, M. J.; Khimyak, Y. Z.; Campbell, N. L.; Kirk, R.; Stockel, E.; Cooper, A. I. *Chem. Mater.* **2007**, *19*, 2034−2048. (c) Ben, T.; Ren, H.; Ma, S. Q.; Cao, D. P.; Lan, J. H.; Jing, X. F.; Wang, W. C.; Xu, J.; Deng, F.; Simmons, J. M.; Qiu, S. L.; Zhu, G. S. *Angew. Chem., Int. Ed.* **2009**, *48*, 9457−9460. (d) Budd, P. M.; Ghanem, B. S.; Makhseed, S.; McKeown, N. B.; Msayib, K. J.; Tattershall, C. E. *Chem. Commun.* **2004**, 230−231.

(7) (a) Rabbani, M. G.; Reich, T. E.; Kassab, R. M.; Jackson, K. T.; El-Kaderi, H. M. *Chem. Commun.* **2012**, *48*, 1141−1143. (b) Xiang, Z. H.; Zhou, X.; Zhou, C. H.; Zhong, S.; He, X.; Qin, C. P.; Cao, D. P. *J. Mater. Chem.* **2012**, *22*, 22663−22669. (c) Katekomol, P.; Roeser, J.; Bojdys, M.; Weber, J.; Thomas, A. *Chem. Mater.* **2013**, *25*, 1542−1548.

(8) (a) Pan, L.; Adams, K. M.; Hernandez, H. E.; Wang, X.; Zheng, C.; Hattori, Y.; Kaneko, K. *J. Am. Chem. Soc.* **2003**, *125*, 3062−3067. (b) Jin, Y.; Voss, B. A.; Jin, A.; Long, H.; Noble, R. D.; Zhang, W. *J. Am. Chem. Soc.* **2011**, *133*, 6650−6658. (c) Lu, W. G.; Yuan, D. Q.; Zhao, D.; Schilling, C. I.; Plietzsch, O.; Muller, T.; Brase, S.; Guenther, J.; Blumel, J.; Krishna, R.; Li, Z.; Zhou, H. C. *Chem. Mater.* **2010**, *22*, 5964−5972.

(9) (a) Laybourn, A.; Dawson, R.; Clowes, R.; Iggo, J. A.; Cooper, A. I.; Khimyak, Y. Z.; Adams, D. J. *Polym. Chem.* **2012**, *3*, 533−537. (b) Sevilla, M.; Valle-Vigón, P.; Fuertes, A. B. *Adv. Funct. Mater.* **2011**, *21*, 2781−2787. (c) Nugent, P.; Belmabkhout, Y.; Burd, S. D.; Cairns, A. J.; Luebke, R.; Forrest, K.; Pham, T.; Ma, S.; Space, B.; Wojtas, L. *Nature* **2013**, *495*, 80−84.

(10) (a) Li, G. Y.; Wang, Z. G. *Macromolecules* **2013**, *46*, 3058−3066. (b) Bae, Y. S.; Snurr, R. Q. *Angew. Chem., Int. Ed.* **2011**, *50*, 11586−11596.

(11) (a) Patel, H. A.; Je, S. H.; Park, J.; Chen, D. P.; Jung, Y.; Yavuz, C. T.; Coskun, A. *Nat. Commun.* **2013**, *4*, 1357. (b) Saleh, M.; Tiwari, J. N.; Kemp, K. C.; Yousuf, M.; Kim, K. S. *Environ. Sci. Technol.* **2013**, *47*, 5467−5473. (c) Chun, J.; Kang, S.; Kang, N.; Lee, S. M.; Kim, H. J.; Son, S. U. *J. Mater. Chem. A* **2013**, *1*, 5517−5523.

(12) (a) Dawson, R.; Cooper, A. I.; Adams, D. J. *Polym. Int.* **2013**, *62*, 345−352. (b) Ma, H. P.; Ren, H.; Zou, X. Q.; Sun, F. X.; Yan, Z. J.; Cai,

K.; Wang, D. Y.; Zhu, G. S. *J. Mater. Chem. A* **2013**, *1*, 752−758. (c) Luo, Y. L.; Li, B. Y.; Wang, W.; Wu, K. B.; Tan, B. *Adv. Mater.* **2012**, *24*, 5703−5707. (d) Hudson, M. R.; Queen, W. L.; Mason, J. A.; Fickel, D. W.; Lobo, R. F.; Brown, C. M. *J. Am. Chem. Soc.* **2012**, *134*, 1970−1973.
(13) Dawson, R.; Stockel, E.; Holst, J. R.; Adams, D. J.; Cooper, A. I. *Energy Environ. Sci.* **2011**, *4*, 4239−4245.
(14) Chen, Q.; Luo, M.; Hammershoj, P.; Zhou, D.; Han, Y.; Laursen, B. W.; Yan, C. G.; Han, B. H. *J. Am. Chem. Soc.* **2012**, *134*, 6084−6087.
(15) (a) Lu, W.; Yuan, D.; Sculley, J.; Zhao, D.; Krishna, R.; Zhou, H.-C. *J. Am. Chem. Soc.* **2011**, *133*, 18126−18129. (b) Lu, W. G.; Sculley, J. P.; Yuan, D. Q.; Krishna, R.; Wei, Z. W.; Zhou, H. C. *Angew. Chem., Int. Ed.* **2012**, *51*, 7480−7484.
(16) (a) Katsoulidis, A. P.; Kanatzidis, M. G. *Chem. Mater.* **2011**, *23*, 1818−1824. (b) Katsoulidis, A. P.; Kanatzidis, M. G. *Chem. Mater.* **2012**, *24*, 471−479.
(17) (a) Rabbani, M. G.; El-Kaderi, H. M. *Chem. Mater.* **2012**, *24*, 1511−1517. (b) Zhao, Y. C.; Cheng, Q. Y.; Zhou, D.; Wang, T.; Han, B. H. *J. Mater. Chem.* **2012**, *22*, 11509−11514. (c) Yu, H.; Tian, M.; Shen, C.; Wang, Z. *Polym. Chem.* **2013**, *4*, 961−968.
(18) (a) Yu, H.; Shen, C. J.; Tian, M. Z.; Qu, J.; Wang, Z. G. *Macromolecules* **2012**, *45*, 5140−5150. (b) Yu, H.; Shen, C.; Wang, Z. *ChemPlusChem* **2013**, *78*, 498−505.
(19) Kuhn, P.; Antonietti, M.; Thomas, A. *Angew. Chem., Int. Ed.* **2008**, *47*, 3450−3453.
(20) Kuhn, P.; Forget, A.; Su, D. S.; Thomas, A.; Antonietti, M. *J. Am. Chem. Soc.* **2008**, *130*, 13333−13337.
(21) (a) Zhang, W.; Li, C.; Yuan, Y. P.; Qiu, L. G.; Xie, A. J.; Shen, Y. H.; Zhu, J. F. *J. Mater. Chem.* **2010**, *20*, 6413−6415. (b) Zhu, X.; Tian, C. C.; Mahurin, S. M.; Chai, S. H.; Wang, C. M.; Brown, S.; Veith, G. M.; Luo, H. M.; Liu, H. L.; Dai, S. *J. Am. Chem. Soc.* **2012**, *134*, 10478−10484. (c) Ren, S. J.; Bojdys, M. J.; Dawson, R.; Laybourn, A.; Khimyak, Y. Z.; Adams, D. J.; Cooper, A. I. *Adv. Mater.* **2012**, *24*, 2357−2361.
(22) (a) Verborgt, J.; Marvel, C. S. *J. Polym. Sci., Polym. Chem. Ed.* **1973**, *11*, 261−73. (b) He, X. H.; Huang, Z. T. *Acta Chim. Sin.* **1984**, *6*, 576−579. (c) Yu, G. P.; Li, B.; Liu, J. L.; Wu, S. F.; Tan, H. J.; Pan, C. Y.; Jian, X. G. *Polym. Degrad. Stab.* **2012**, *97*, 1807−1814.
(23) Bhunia, A.; Vasylyeva, V.; Janiak, C. *Chem. Commun.* **2013**, *49*, 3961−3963.
(24) Kuhn, P.; Thomas, A.; Antonietti, M. *Macromolecules* **2009**, *42*, 319−326.
(25) Bojdys, M. J.; Jeromenok, J.; Thomas, A.; Antonietti, M. *Adv. Mater.* **2010**, *22*, 2202−2205.
(26) Bhunia, A.; Boldog, I.; Möller, A.; Janiak, C. *J. Mater. Chem. A* **2013**, *1*, 14990−14999.
(27) Zhao, Y.; Yao, K. X.; Teng, B.; Zhang, T.; Han, Y. *Energy Environ. Sci.* **2013**, *6*, 3684−3692.
(28) Britt, D.; Furukawa, H.; Wang, B.; Glover, T. G.; Yaghi, O. M. *Proc. Natl. Acad. Sci. U. S. A.* **2009**, *106*, 20637−20640. (b) Yazaydin, A. O.; Snurr, R. Q.; Park, T. H.; Koh, K.; Liu, J.; LeVan, M. D.; Benin, A. I.; Jakubczak, P.; Lanuza, M.; Galloway, D. B.; Low, J. J.; Willis, R. R. *J. Am. Chem. Soc.* **2009**, *131*, 18198−18199.
(29) Plietzsch, O.; Schilling, C. I.; Grab, T.; Grage, S. L.; Ulrich, A. S.; Comotti, A.; Sozzani, P.; Muller, T.; Bräse, S. *New J. Chem.* **2011**, *35*, 1577−1581.
(30) (a) Schmidt, J.; Werner, M.; Thomas, A. *Macromolecules* **2009**, *42*, 4426−4429. (b) Zhang, K.; Tieke, B.; Vilela, F.; Skabara, P. J. *Macromol. Rapid Commun.* **2011**, *32*, 825−830.
(31) (a) McKeown, N. B.; Gahnem, B.; Msayib, K. J.; Budd, P. M.; Tattershall, C. E.; Mahmood, K.; Tan, S.; Book, D.; Langmi, H. W.; Walton, A. *Angew. Chem., Int. Ed.* **2006**, *45*, 1804−1807. (b) Wood, C. D.; Tan, B.; Trewin, A.; Su, F.; Rosseinsky, M. J.; Bradshaw, D.; Sun, Y.; Zhou, L.; Cooper, A. I. *Adv. Mater.* **2008**, *20*, 1916−1921. (c) Du, N.; Robertson, G. P.; Pinnau, I.; Guiver, M. D. *Macromolecules* **2009**, *42*, 6023−6030.
(32) Zou, X.; Ren, H.; Zhu, G. *Chem. Commun.* **2013**, *49*, 3925−3936.
(33) Liebl, M. R.; Senker, J. R. *Chem. Mater.* **2013**, *25*, 970−980.
(34) Kandambeth, S.; Mallick, A.; Lukose, B.; Mane, M. V.; Heine, T.; Banerjee, R. *J. Am. Chem. Soc.* **2012**, *134*, 19524−19527.
(35) (a) Lan, J. H.; Cao, D. P.; Wang, W. C.; Ben, T.; Zhu, G. S. *J. Phys. Chem. Lett.* **2010**, *1*, 978−981. (b) Garibay, S. J.; Weston, M. H.; Mondloch, J. E.; Colon, Y. J.; Farha, O. K.; Hupp, J. T.; Nguyen, S. T. *CrystEngComm* **2013**, *15*, 1515−1519. (c) El-Kaderi, H. M.; Hunt, J. R.; Mendoza-Cortes, J. L.; Cote, A. P.; Taylor, R. E.; O'Keeffe, M.; Yaghi, O. M. *Science* **2007**, *316*, 268−272. (d) Yu, J. T.; Chen, Z.; Sun, J. L.; Huang, Z. T.; Zheng, Q. Y. *J. Mater. Chem.* **2012**, *22*, 5369−5373.
(36) (a) Wang, Z.; Yuan, S. W.; Mason, A.; Reprogle, B.; Liu, D. J.; Yu, L. P. *Macromolecules* **2012**, *45*, 7413−7419. (b) Tsyurupa, M. P.; Davankov, V. A. *React. Funct. Polym.* **2006**, *66*, 768−779.
(37) Lim, H.; Cha, M. C.; Chang, J. Y. *Macromol. Chem. Phys.* **2012**, *213*, 1385−1390.
(38) Ma, J. P.; Wang, M.; Du, Z. T.; Chen, C.; Gao, J.; Xu, J. *Polym. Chem.* **2012**, *3*, 2346−2349.
(39) Jackson, K. T.; Rabbani, M. G.; Reich, T. E.; El-Kaderi, H. M. *Polym. Chem.* **2011**, *2*, 2775−2777.
(40) Xiang, Z. H.; Cao, D. P. *J. Mater. Chem. A* **2013**, *1*, 2691−2718.
(41) Shen, C. J.; Bao, Y. J.; Wang, Z. G. *Chem. Commun.* **2013**, *49*, 3321−3323.
(42) (a) Zhou, H.; Xu, S.; Su, H.; Wang, M.; Qiao, W.; Ling, L.; Long, D. *Chem. Commun.* **2013**, *49*, 3763−3765. (b) McDonald, T. M.; D'Alessandro, D. M.; Krishna, R.; Long, J. R. *Chem. Sci.* **2011**, *2*, 2022−2028.
(43) Martin, C. F.; Stockel, E.; Clowes, R.; Adams, D. J.; Cooper, A. I.; Pis, J. J.; Rubiera, F.; Pevida, C. *J. Mater. Chem.* **2011**, *21*, 5475−5483.
(44) (a) Li, B.; Gong, R.; Luo, Y.; Tan, B. *Soft Mater.* **2011**, *7*, 10910−10916. (b) Dawson, R.; Adams, D. J.; Cooper, A. I. *Chem. Sci.* **2011**, *2*, 1173−1177. (c) Ding, S. Y.; Wang, W. *Chem. Soc. Rev.* **2013**, *42*, 548−568. (d) Xu, C.; Hedin, N. *J. Mater. Chem. A* **2013**, *1*, 3406−3414.
(45) (a) Li, B.; Gong, R.; Wang, W.; Huang, X.; Zhang, W.; Li, H.; Hu, C.; Tan, B. *Macromolecules* **2011**, *44*, 2410−2414. (b) Liu, Y. L.; Eubank, J. F.; Cairns, A. J.; Eckert, J.; Kravtsov, V. C.; Luebke, R.; Eddaoudi, M. *Angew. Chem., Int. Ed.* **2007**, *46*, 3278−3283. (c) Vaidhyanathan, R.; Iremonger, S. S.; Dawson, K. W.; Shimizu, G. K. *Chem. Commun.* **2009**, 5230−5232.
(46) (a) Ben, T.; Li, Y. Q.; Zhu, L. K.; Zhang, D. L.; Cao, D. P.; Xiang, Z. H.; Yao, X. D.; Qiu, S. L. *Energy Environ. Sci.* **2012**, *5*, 8370−8376. (b) Lu, W. G.; Yuan, D. Q.; Sculley, J. L.; Zhao, D.; Krishna, R.; Zhou, H. C. *J. Am. Chem. Soc.* **2011**, *133*, 18126−18129.
(47) (a) Ren, S.; Dawson, R.; Laybourn, A.; Jiang, J. X.; Khimyak, Y.; Adams, D. J.; Cooper, A. I. *Polym. Chem.* **2012**, *3*, 928−934. (b) Zheng, B. S.; Yang, Z.; Bai, J. F.; Li, Y. H.; Li, S. H. *Chem. Commun.* **2012**, *48*, 7025−7027. (c) Mohanty, P.; Kull, L. D.; Landskron, K. *Nat. Commun.* **2011**, *27*, 401−402.
(48) Frost, H.; Duren, T.; Snurr, R. Q. *J. Phys. Chem. B* **2006**, *110*, 9565−9570.
(49) (a) Furukawa, H.; Yaghi, O. M. *J. Am. Chem. Soc.* **2009**, *131*, 8875−8883. (b) Makhseed, S.; Samuel, J. *Chem. Commun.* **2008**, 4342−4344. (c) Makhseed, S.; Samuel, J. *J. Mater. Chem. A* **2013**, *1*, 13004−13010.